Biochemistry

 Volume 39, Number 6 February 15, 2000

Articles

Kinetic Studies of the Mechanism of Carbon−Hydrogen Bond Breakage by the Heterotetrameric Sarcosine Oxidase of *Arthrobacter* sp. 1-IN[†]

Richard J. Harris,[‡] Rolandas Meskys,[§] Michael J. Sutcliffe,[||] and Nigel S. Scrutton*,[‡]

Department of Biochemistry and Department of Chemistry, University of Leicester, University Road, Leicester LE1 7RH, U.K., and Sector of Biosynthesis, Laboratory of Bioanalysis, Institute of Biochemistry, Mokslininku 12, 2600 Vilnius, Lithuania

Received August 19, 1999; Revised Manuscript Received November 2, 1999

ABSTRACT: The reaction of heterotetrameric sarcosine oxidase (TSOX) of *Arthrobactor* sp. 1-IN has been studied by stopped-flow spectroscopy, with particular emphasis on the reduction of the enzyme by sarcosine. Expression of the cloned gene encoding TSOX in *Escherichia coli* enables the production of TSOX on a scale suitable for stopped-flow studies. Treatment of the enzyme with sulfite provides the means for selective formation of a flavin−sulfite adduct with the covalent 8α-(N^3-histidyl)-FMN. Formation of the sulfite−flavin adduct suppresses internal electron transfer between the noncovalent FAD (site of sarcosine oxidation) and the covalent FMN (site of enzyme oxidation) and thus enables detailed characterization of the kinetics of FAD reduction by sarcosine using stopped-flow methods. The rate of FAD reduction displays a simple hyperbolic dependence on sarcosine concentration. Studies in the pH range 6.5−10 indicate there are no kinetically influential ionizations in the enzyme−substrate complex. A plot of the limiting rate of flavin reduction/the enzyme−substrate dissociation constant (k_{lim}/K_d) versus pH is bell-shaped and characterized by two macroscopic pK_a values of 7.4 ± 0.1 and 10.4 ± 0.2: potential candidates for the two ionizable groups are discussed with reference to the structure of monomeric sarcosine oxidase (MSOX). The kinetic data are discussed with reference to potential mechanisms for the oxidation of amine molecules by flavoenzymes. Additionally, kinetic isotope effect studies of the rate of C−H bond breakage suggest that a ground-state quantum tunneling mechanism for H-transfer, facilitated by the low-frequency thermal motions of the protein molecule, accounts for C−H bond cleavage by TSOX. TSOX thus provides another example of C−H bond breakage by ground-state quantum tunneling, driven by protein dynamics [vibrationally enhanced ground-state quantum tunneling (VEGST)], for the oxidation of amines by enzymes.

Sarcosine oxidase (SOX;[1] EC 1.5.3.1) catalyzes the oxidative demethylation of sarcosine to produce glycine and formaldehyde:

$$CH_3NHCH_2COOH + O_2 + H_2O \rightarrow HCHO + NH_2CH_2COOH + H_2O_2$$

The enzyme has been isolated from various organisms, and the genes encoding SOX have been cloned from bacterial

[†] This work was funded by grants from the Biotechnology and Biological Sciences Research Council, the Royal Society, and the Lister Institute of Preventive Medicine. N.S.S. is a Lister Institute Research Fellow.

* Correspondence should be addressed to this author at the Department of Biochemistry, University of Leicester, University Rd., Leicester LE1 7RH, U.K. Telephone: +44 116 223 1337. Telefax: +44 116 252 3369. Email: nss4@le.ac.uk.

[‡] Department of Biochemistry, University of Leicester.

[§] Laboratory of Bioanalysis, Institute of Biochemistry.

[||] Department of Chemistry, University of Leicester.

[1] Abbreviations: SOX, sarcosine oxidase; MSOX, monomeric sarcosine oxidase; DSOX, heterodimeric sarcosine oxidase; TSOX, heterotetrameric sarcosine oxidase; PIPOX, pipecolate oxidase; DMGDH, dimethylglycine dehydrogenase; SDH, sarcosine dehydrogenase.

10.1021/bi991941v CCC: $19.00
Published on Web 01/20/2000

(*1*−*4*) and eukaryotic (*5*) sources. SOX belongs to a larger family of enzymes including *N*-methyltryptophan oxidase (MTOX), pipecolate oxidase (PIPOX), dimethylglycine dehydrogenase (DMGDH), and sarcosine dehydrogenase (SDH), which catalyze similar oxidative demethylation reactions of secondary and tertiary amino acids. The bacterial SOX enzymes are induced in various microorganisms when grown on sarcosine as the sole source of carbon and energy. These bacterial enzymes can be divided into three subclasses: the monomeric (MSOX), the heterodimeric (DSOX), and the heterotetrameric (TSOX) enzymes. MSOX from *Bacillus* sp. B-0618 has been cloned and shown to have a molecular mass of 43.8 kDa (*1*) and to contain a covalently attached flavin in the form of an 8α-*S*-cysteinyl linkage to Cys-315 (*6*); this covalent link is conserved in the related MTOX and PIPOX enzymes. The crystallographic structure of MSOX has been solved at 2.0 Å resolution (*6*), revealing a two-domain protein with an overall topology similar to D-amino acid oxidase (*7*). MSOX exhibits approximately 20−25% sequence identity with the *β*-subunit of *Corynebacterial* TSOX (*3*). TSOX contains four different subunits of approximate molecular masses 100, 45, 21, and 11 kDa (*8*) and also contains noncovalently bound FAD, noncovalently bound NAD^+ (*9*), and covalently bound FMN attached to the *β*-subunit [residue His-173 of the *Corynebacterial* TSOX; (*10*)] in the form of 8α-(N^3-histidyl)-FMN (*11*). TSOX also contains two sites for tetrahydrofolate (H_4folate). H_4folate does not affect the rate of sarcosine oxidation, but reactions performed in the presence of H_4folate yield methylenetetrahydrofolate rather than formaldehyde (*12*). No crystallographic structure exists for a bacterial TSOX.

The catalytic and spectroscopic properties of *Corynebacterial* TSOX have been investigated already. Both flavins are reducible with sarcosine or dithionite, and two electrons per flavin are required for complete reduction; the blue neutral flavin semiquinone is observed during the course of reductive titration (*13*). Sarcosine dehydrogenation occurs at the noncovalent flavin, whereas the oxidase activity is associated with the covalently bound flavin. Sulfite inhibits oxidase activity (but does not prevent enzyme reduction with sarcosine) by forming a reversible covalent complex with the 8α-(N^3-histidyl)-FMN (*13*). Combined UV−visible and EPR spectroscopy studies have demonstrated that comproportionation of the substrate-reduced noncovalent dihydroflavin produces a biradical form of TSOX comprising a 50:50 mixture of red anionic and blue neutral flavin semiquinones (*14*). Rapid mixing stopped-flow and pH-jump studies have shown that TSOX cycles predominantly between the oxidized and 2-electron reduced forms during steady-state reactions and that 2-electron reduction of the enzyme by sarcosine is rate-limiting (45 s^{-1} at pH 8.0). Reaction of 2-electron reduced TSOX with oxygen is 1.7-fold faster (75 s^{-1}) than the aerobic turnover rate, and the pH-jump technique was used to demonstrate that intramolecular electron transfer between the two flavins is fast (750 s^{-1} at pH 8.0) (*15*).

In this paper, we have investigated the pH dependence and temperature dependence of the rate of reduction by sarcosine of the noncovalent flavin in the TSOX of *Arthrobacter* sp. 1-IN. Our studies demonstrate two kinetically influential ionizations in the free enzyme and/or free substrate of pK_a values 7.4 ± 0.1 and 10.4 ± 0.2. No kinetically influential ionizations were observed in the ES complex formed between TSOX and sarcosine over the pH range investigated. These studies are consistent with proposed mechanisms for the oxidation of amine substrates by flavoenzymes, including the so-called carbanion mechanism, direct hydride transfer mechanism, or mechanisms involving homolysis of the C−H bond (e.g., see refs *16* and *17*). Studies of the temperature dependence of the flavin reduction rate with sarcosine and *N*-methyl-d_3-glycine (deuterated sarcosine) indicate a nonclassical mode of breaking the substrate C−H bond, and strongly suggest that vibrationally enhanced ground-state tunneling [VEGST (*18, 19*)] of hydrogen occurs during breakage of the substrate C−H bond.

EXPERIMENTAL PROCEDURES

Chemicals and Enzymes. Complex bacteriological media were from Unipath, and all media were prepared as described by Sambrook et al. (*20*). Sarcosine (HCl salt), NAD^+, FAD, *o*-dianisidine, and horseradish peroxidase were from Sigma. *N*-Methyl-d_3-glycine hydrochloride (deuterated sarcosine) was from CK Gas Products Ltd. All other chemicals were of analytical grade where possible.

Isolation of Recombinant Arthrobacter TSOX. Standard cloning methods were as described elsewhere (*20*). Cloning of the genes encoding TSOX from *Arthrobacter* sp. 1-IN has been described previously (*21*). Sequence analysis has established that the TSOX from this strain is 96% identical with the TSOX of *Corynebacterium* sp. P-1 (Harris, Meskys, and Scrutton, unpublished) and that the gene order within the *sox* operon is identical to that described for the *Corynebacterial* enzyme. Overexpression of the *sox* genes was accomplished by subcloning the whole of the *sox* operon into the plasmid vector pET-11d where the genes come under the control of the T7 promoter. To achieve expression, the *sox* operon was originally isolated as a 12 kb fragment cloned into plasmid pTZ18R (*21*). The operon was released from plasmid pTZ18R by digestion with the restriction enzymes *Hin*dIII and *Kpn*I to generate 7.5 kb *sox* operon-containing DNA fragment. The first gene in the operon (*sox* B) contains an *Nco*I site at the position of the initiating methionine, and a second *Nco*I site is located at the beginning of the *sox* D gene (the subsequent gene in the operon). The 7.5 kb *Hin*dIII/*Kpn*I fragment was thus partially digested with *Nco*I and the *sox* operon cloned into plasmid pET-11d as a 6.5 kb *Nco*I/*Hin*dIII fragment. The resultant construct was designated pSOX. Recombinant TSOX was isolated by transforming plasmid pSOX into *E. coli* strain BL21/DE3. Transformed cells were grown in 2× YT media (10 L) containing 50 μg/mL Timentin at 21 °C until stationary phase was reached. Cells were harvested by centrifugation, resuspended in 50 mM potassium phosphate buffer, pH 7.3 (buffer A), and broken by passage through a French press (140 MPa). Membranes were removed by centrifugation (15000*g*) for 15 min, and the supernatant was fractionated with ammonium sulfate, while maintaining the pH at 7.3 by the addition of K_2HPO_4 as required. The 30−50% ammonium sulfate fraction was harvested by centrifugation (15000*g*) for 20 min, dialyzed exhaustively against 20 mM potassium phosphate buffer, pH 7.3 (buffer B), and then applied to an anion exchange column (DE-52; 5.5 cm × 12 cm) equilibrated with the same buffer. After the column was washed with 0.15 M KCl contained in buffer B, the column was developed using a gradient (0.15−0.6 M) of KCl contained in buffer B.

TSOX-containing fractions were pooled, concentrated to about 10 mL by ultrafiltration, and made 1 M with respect to ammonium sulfate. The enzyme was applied to a column (3 cm × 10 cm) of phenyl Sepharose equilibrated with buffer B containing 1 M ammonium sulfate. The column was developed by the application of a 1−0 M ammonium sulfate gradient contained in buffer B. Fractions containing TSOX were pooled, dialyzed exhaustively against 20 mM Tris-HCl, pH 8.0 (buffer C), and applied to a Q-Sepharose (HP) fast flow column (2.5 cm × 2.5 cm) equilibrated with buffer C. TSOX was eluted using a KCl gradient (0−0.6 M) contained in buffer C. TSOX was exchanged into buffer B by exhaustive dialysis and concentrated to about 10 mg/mL for storage at −20 °C.

Methods of Protein Analysis. The presence of FAD and NAD^+ in purified TSOX was confirmed by reverse-phase hplc analysis using a Waters Spherisorb S5 ODS2 reverse-phase column. The column was equilibrated with 80% 50 mM potassium phosphate, pH 6.5/20% methanol. Samples of enzyme were boiled for 5 min to release cofactors, and protein was removed by microcentrifugation for 10 min. Following sample application, cofactors were eluted using a 20−100% methanol gradient. Authentic samples of FAD, FMN, AMP, and NAD^+ were used as standards. Covalent linkage of flavin to the TSOX β-subunit was demonstrated by separating the subunits by SDS−polyacrylamide gel electrophoresis and detection of flavin fluorescence following exposure of the gel to UV light (*22*). The concentration of TSOX was determined from the flavin absorbance [ϵ_{450} = 12 700 M^{-1} cm^{-1}; (*8*)] and calculated on the basis of 2 mol of flavin/mol of TSOX.

Steady-State Kinetic Analysis. Steady-state kinetic measurements were performed with a 1 cm light path in a final volume of 1 mL at 25 °C. The reaction mixture contained 5 IU of horseradish peroxidase, 0.007% w/w *o*-dianisidine contained in 20 mM potassium phosphate buffer, pH 8.5. The desired concentrations of sarcosine and enzyme were obtained by making microliter additions from stock solutions to the assay mixture. Reactions were initiated by the addition of substrate, and the increase in absorbance at 430 nm due to oxidation of *o*-dianisidine ($\epsilon_{430} = 1.08 \times 10^4$ M^{-1} cm^{-1}) was measured using a Hewlett-Packard 8452A diode array spectrophotometer.

Stopped-Flow Spectroscopy. Rapid kinetic experiments were performed using an Applied Photophysics SX17MV and SX18MV stopped-flow spectrophotometer. Time-dependent reduction of TSOX was performed using diode array detection or single-wavelength detection as necessary. For diode array studies, spectral deconvolution was performed by global analysis and numerical integration methods using PROKIN software (Applied Photophysics). For single-wavelength studies, data collected at 450 nm were analyzed using nonlinear least-squares regression on an Archimedes 410-1 microcomputer using Spectrakinetics software (Applied Photophysics). Experiments were performed by mixing sulfite-treated TSOX (see Results) in buffer of the desired pH, with an equal volume of sarcosine at the desired concentration in the same buffer. In pH and temperature dependence studies, the concentration of substrate was always at least 10-fold greater than that of TSOX, thereby ensuring pseudo-first-order conditions. For each substrate concentration used, at least four replicate measurements were collected and averaged. Absorbance changes at 450 nm were either biphasic (transients were analyzed using a two-exponential expression) or monophasic (transients fitted to a single-exponential expression). The observed rate constants for monophasic transients and for the fast phase (flavin reduction) of biphasic transients were found to exhibit a hyperbolic dependence on substrate concentration, and the reaction sequence was modeled as shown in the general scheme involving the establishment of a rapid equilibrium between the ES complex and free enzyme and substrate forms prior to flavin reduction:

$$E_{ox} + \text{sarcosine} \leftrightarrow E_{ox}\cdot\text{sarcosine} \rightarrow E_{red} + P \quad (1)$$

Data were then fitted to obtain related K_d and k_{lim} values using eq 2 (*23*):

$$k_{obs} = k_{lim}[S]/(K_d + [S]) \quad (2)$$

The pH profile for the kinetic parameter k_{lim}/K_d was constructed, and data were fitted using eq 3:

$$k_{lim}/K_d = T_{max}/(1 + 10^{(pK_{a1}-pH)} + 10^{(pH-pK_{a2})}) \quad (3)$$

T_{max} is the theoretical maximal value of k_{lim}/K_d.

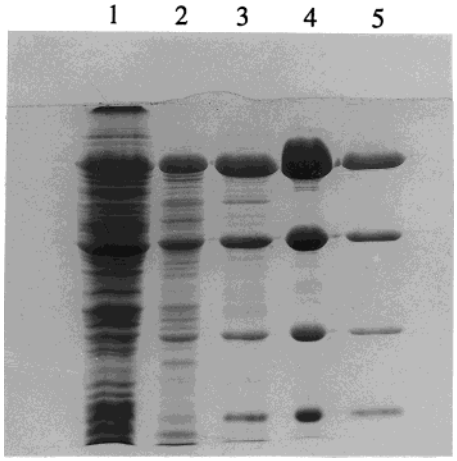

FIGURE 1: SDS−polyacrylamide gel electrophoretic analysis of the purification of recombinant TSOX from *E. coli* strain BL21/DE3 transformed with pSOX. Lane 1, sample of broken cells following breakage with a French press; lane 2, fraction obtained following ammonium sulfate fractionation; lane 3, pooled fractions following ion-exchange chromatography (DE-52); lane 4, pooled fractions obtained following hydrophobic interaction chromatography (phenyl Sepharose); lane 5, pooled fractions following chromatography using Q-Sepharose (HP).

RESULTS

Expression and Purification of Recombinant TSOX and Titration with Sulfite. TSOX was expressed at high levels in *E. coli* strain BL21/DE3 transformed with plasmid pSOX. The enzyme was purified to homogeneity and in high yield (300 mg from a 10 L culture of the recombinant *E. coli* strain) using the procedure described above (Figure 1). The UV−visible spectrum of recombinant TSOX resembled that of native enzyme purified from *Arthrobacter* sp. 1-IN (Figure 2, spectrum 1). This situation is in contrast to the *Corynebacterial* recombinant TSOX, which is purified in a form containing a covalent and reversible cysteine−flavin C4a adduct (*24*). The cofactor content of recombinant *Arthro-*

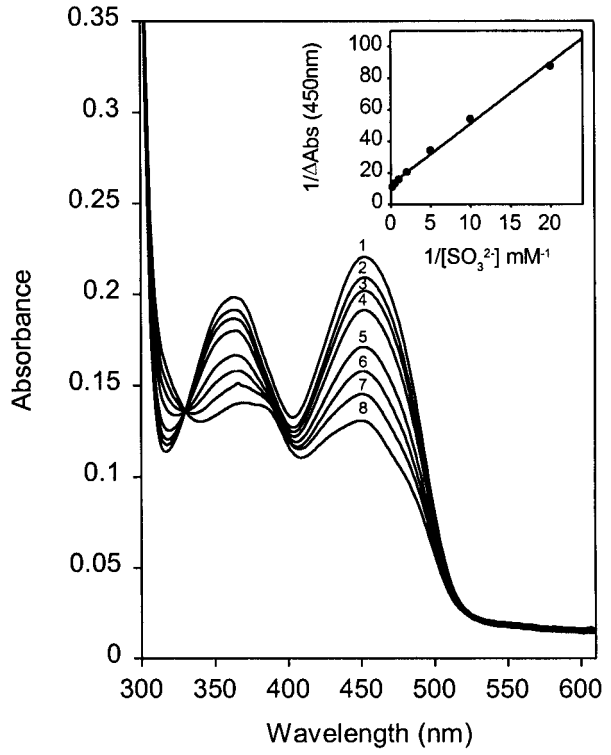

FIGURE 2: Titration of sarcosine oxidase with sulfite. Conditions: 20 mM sodium pyrophosphate buffer, pH 8.5, 200 mM KCl at 25 °C. Inset: Plot of $1/\Delta A_{450}$ versus $1/[SO_3^{2-}]$, K_d = 333 μM. Spectrum 1, oxidized TSOX (16 μM); spectra 2−8 inclusive, following addition of sodium sulfite at a final concentration of 50 μM, 100 μM, 200 μM, 500 μM, 1 mM, 6 mM, and 10 mM, respectively. Adduct dissociation constants (shown in parentheses) were also obtained by titration at different pH values: pH 6.5 (71 μM), pH 7.0 (95 μM), pH 8.0 (230 μM), pH 9.0 (4.6 mM), pH 10.0 (10 mM). Buffers used were 20 mM potassium phosphate (pH 6.5 and 7.0), 20 mM sodium pyrophosphate (pH 8.0), 20 mM sodium borate (pH 9.0 and 10.0).

Scheme 1 : Kinetic Scheme for the Reduction of TSOX by Sarcosine

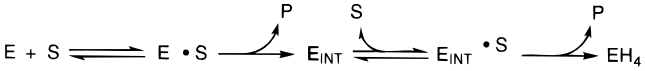

bacter sp. 1-IN TSOX was shown to be identical to that of *Corynebacterial* TSOX using the methods described above. Using the coupled assay system described above, the specific activity of purified recombinant *Arthrobacter* TSOX was calculated to be 1.2 μmol of *o*-dianisidine oxidized min^{-1} (mg of TSOX)$^{-1}$.

Previous studies with the *Corynebacterial* TSOX have shown that sulfite selectively forms a reversible adduct with the 8α-(*N*^{3}-histidyl)-FMN resulting in inhibition of the oxidase activity of the enzyme (*13*). Treatment with sulfite does not prevent reduction of the sulfite-unreactive flavin by sarcosine. Electron transfer in *Corynebacterial* TSOX has been shown to proceed by the mechanism shown in Scheme 1 (*15*). Stopped-flow studies in which sarcosine is mixed with TSOX give rise to complex spectral changes. These reflect initial production of the 2-electron reduced enzyme[2] (E_{INT}; observed at long wavelength, indicating the formation of a flavin neutral semiquinone species) followed by complete reduction to the 4-electron reduced species of TSOX (EH_4). Rapid equilibrium conditions apply to the binding steps shown in Scheme 1 (*15*). Stopped-flow studies of reduction of the noncovalent flavin by sarcosine are thus complicated by spectral changes occurring as a result of multiple turnover and internal electron transfer within TSOX. However, as shown here for the *Arthrobacter* enzyme (see below) and by other workers for the *Corynebacterial* enzyme (*25*), studies of FAD reduction can be simplified by treatment of TSOX with sulfite. Formation of the reversible covalent adduct prevents internal electron transfer from the noncovalent FAD to the 8α-(*N*^{3}-histidyl)-FMN, and thus the enzyme is able to accept only 2 electrons from substrate; i.e., the reaction is restricted to a single-turnover situation. In developing a simplified stopped-flow procedure for studying FAD reduction in the TSOX of *Arthrobacter* sp. 1-IN, the sulfite reactivity of the enzyme was investigated. As expected, treatment with sulfite elicits spectral changes consistent with adduct formation at the 8α-(*N*^{3}-histidyl)-FMN (Figure 2). Similarly, sulfite titrations were performed over the entire pH range used in the stopped-flow studies described below and the corresponding adduct dissociation constants calculated (Figure 2). Addition of sarcosine to sulfite-treated enzyme demonstrated that sulfite treatment did not affect the ability of the enzyme to be reduced by sarcosine. This addition of sarcosine effected a spectral change—manifested by further reduction in the absorption at 450 nm—similar to that reported previously for the *Corynebacterial* enzyme [data not shown; (*13*)].

Stopped-Flow Studies of FAD Reduction in Sulfite-Treated TSOX. The reductive half-reaction of sulfite-treated TSOX was studied by stopped-flow spectroscopy at 25 °C. Given the relatively high sarcosine concentrations used in this study, there is a potential concern regarding ionic strength effects on the observed kinetic behavior. Consequently, the total ionic strength was kept constant by balancing with KCl the contribution made by sarcosine.

Enzyme reduction was followed by photodiode array detection, and data were fitted globally using numerical integration methods using Prokin software (Applied Photophysics). Initial experiments were performed with equal molar quantities of TSOX and sarcosine to assess the efficacy of sulfite treatment in suppressing oxidase activity. Data collected over 200 s after mixing were best fit to a two-step model:

$$A \rightarrow B \rightarrow C$$

Species A represents the oxidized form of sulfite-treated TSOX (Figure 3). The calculated spectral forms indicated that species B is a 2-electron-reduced form of sulfite-treated TSOX (as revealed by the large reduction in absorption at 450 nm). Species C is an alternate form of reduced sulfite-treated TSOX in which the 450 nm absorption is reduced further—whether the slow phase reflects further reduction of the FAD remains to be established. This species forms relatively slowly, but the reason for its slow formation is unknown. However, it is worth noting that this reaction was

[2] E_{INT} is a species of TSOX in which both forms of the flavin are reduced at the level of 1 electron. Its formation involves 2-electron reduction of the noncovalent FAD by sarcosine followed by the transfer of 1 electron to the covalent 8α-(*N*^{3}-histidyl)-FMN. Internal electron transfer from FAD to 8α-(*N*^{3}-histidyl)-FMN in TSOX is under prototropic control and is fast compared with FAD reduction by sarcosine (*15*). In stopped-flow experiments, therefore, internal electron transfer is not resolved from reduction of FAD by substrate.

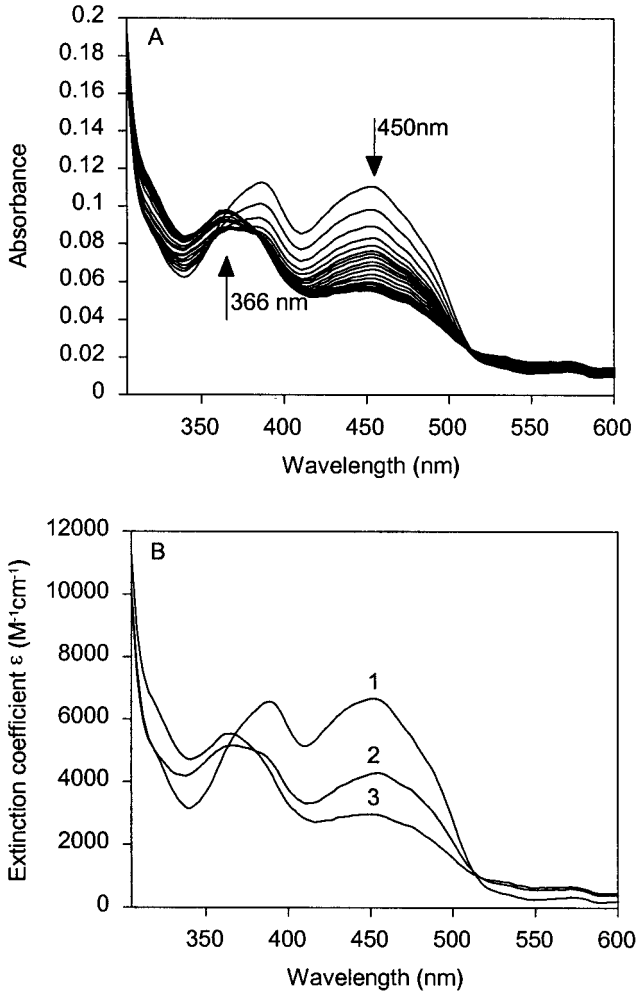

FIGURE 3: Reaction of sulfite-treated TSOX with sarcosine monitored by stopped-flow photodiode array spectroscopy. Conditions: 20 mM sodium pyrophosphate buffer, pH 8.5, 20 mM sodium sulfite, 180 mM KCl, 16.5 μM sulfite-treated TSOX, 16.5 μM sarcosine, 25 °C. Panel A: Time-dependent spectral changes on rapidly mixing sulfite-treated TSOX with sarcosine. The experiment was conducted over 260 s after the initial mixing event. The first spectrum is recorded 1.3 s after mixing; for clarity, only selected subsequent spectra are shown. Panel B: Deconvoluted spectra for the reaction shown in panel A. The data shown in panel A were fitted to the model: A → B → C. Spectrum 1, sulfite-treated TSOX (species A); spectrum 2, enzyme species (B) following the fast phase of the reductive half-reaction; spectrum 3, enzyme species (C) following the slow phase of the reductive half-reaction.

not performed under pseudo-first-order conditions; thus, a change in the rate-determining step (from a first-order reduction step to a second-order binding step) could potentially account for the observed biphasic flavin reduction kinetics. Arguing against this explanation, however, is that biphasic kinetics are also observed under pseudo-first-order conditions (i.e. when [sarcosine] is at least 10-fold that of [TSOX]; see below), thereby negating rate limitation through a second-order binding process.

With equimolar sarcosine, at much longer time excursions (>1000 s), a fourth intermediate forms[3] (form D). Intermediate D is a consequence of the reversible binding of sulfite

[3] The spectral form of species D is not shown since its formation is not complete within 1000 s of the mixing event. Data acquisition beyond 1000 s is not possible using the commercial software used to drive stopped-flow experiments with photodiode array detection.

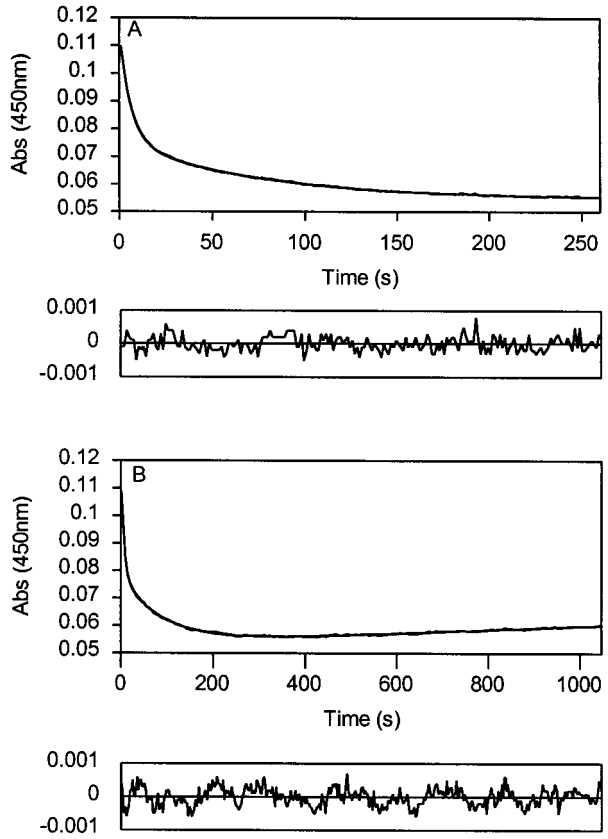

FIGURE 4: Reaction of sulfite-treated TSOX with sarcosine monitored by single-wavelength stopped-flow spectroscopy. Conditions as in Figure 3. Panel A: Transient obtained at 450 nm illustrating the biphasic nature of the reductive transient observed at this wavelength. Panel B: As for panel A, but measurement extended to a longer time excursion to illustrate the partial reoxidation of 2-electron reduced sulfite-treated TSOX by molecular oxygen. The transients demonstrate that the reductive and oxidative phases of the reactions are well resolved.

to the covalent flavin (the site of oxidation) in TSOX. Thus, following prolonged incubation after mixing, molecular oxygen is able to remove electrons from the enzyme following internal electron transfer to the 8α-(N^3-histidyl)-FMN. The data reveal that the presence of sulfite substantially inhibits enzyme reoxidation [by suppressing internal electron transfer from 2-electron reduced FAD to the sulfite-bound 8α-(N^3-histidyl)-FMN] to the extent that the reductive phase of the reaction sequence is clearly resolved from the oxidative phase. Sulfite treatment is therefore effective in suppressing the oxidase activity of TSOX, making studies of flavin reduction by sarcosine possible using the stopped-flow technique.

Consistent with the multiple-wavelength analysis of enzyme reduction, single-wavelength stopped-flow measurements of equimolar mixtures of TSOX and sarcosine demonstrated that reductive transients at 450 nm were biphasic (Figure 4A). Again, after the initial reduction of the enzyme, and following prolonged incubation, the absorption at 450 nm was found to increase again due to enzyme reoxidation (Figure 4B). The fast phase of the reductive transient contributes ~70% of the total absorption change, consistent with electron transfer to the flavin. This phase also reports on C−H bond cleavage, since there is a pronounced kinetic isotope effect (KIE) on this phase (see below).

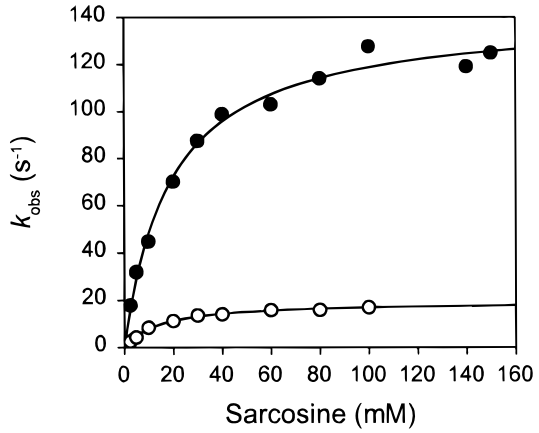

FIGURE 5: Concentration dependence of the observed rate for flavin reduction in sulfite-treated TSOX. Reaction conditions as described in the legend to Figure 3. The total ionic strength at different concentrations of sarcosine was balanced with KCl. Filled circles, reactions performed with sarcosine (k_{lim} 141 s^{-1}, K_d 13.2 mM); open circles, reactions performed with *N*-methyl-d_3-glycine hydrochloride (deuterated sarcosine) (k_{lim} 19.5 s^{-1}, K_d 14.4 mM). Data were fitted using eq 2.

Under pseudo-first-order conditions, the observed rate constant for the fast phase (flavin reduction) was found to be hyperbolically dependent on sarcosine concentration at all pH values studied (Figure 5), which is consistent with the formation of a Michaelis complex prior to reduction of the enzyme-bound FAD. The kinetic scheme shown in eq 1 for enzyme reduction is therefore appropriate, and the concentration dependence of the fast phase can be analyzed using the Strickland equation (eq 2). No lag phase was apparent in the reductive transient, suggesting that the rapid equilibrium assumption is valid. The observed rate constant for the reductive slow phase is independent of sarcosine concentration ($\sim$ 6 s^{-1} at pH 8.5 and 25 °C) over the concentration range studied (2.5−140 mM sarcosine). In pH-dependent and substrate-dependent studies, the slow phase was observed only at pH values of 6.5−8.5, and this phase was more clearly resolved at lower sarcosine concentrations. At high sarcosine concentrations, the transients were monophasic. Additionally, at pH values of 9 and above, the reductive transients were monophasic at all sarcosine concentrations investigated due to loss of the slow phase. The nature of the slow phase remains elusive, and was not investigated further herein. Below we report on a detailed analysis of the fast phase (which shows a large KIE) as a function of solution pH and temperature.

Reduction of FAD by sarcosine was studied over the pH range 6.5−10.5. Sarcosine is zwitterionic at almost all the pH values used in this study.[4] Values for the limiting rate of flavin reduction (k_{lim}) and the dissociation constant for the ES complex (K_d) were calculated between the pH range 6.5 and 10.5 by fitting the data to the hyperbolic equation: $k_{obs1} = k_{lim}[S]/(K_d + [S])$. The pH dependence of k_{lim} and K_d is shown in Figure 6 and the determined kinetic parameters are given in Table 1. Over the pH range studied, k_{lim} is essentially independent of solution pH, revealing the lack of kinetically influential ionizations in the enzyme−substrate complex. At the low end of the pH range studied (pH 6.5 and 7.0), the errors associated with the determined values of k_{lim} are high. These large errors reflect the large values of K_d which lead to poor definition of the hyperbola under these conditions. The pH profile of k_{lim}/K_d is bell-shaped. Data fitting using eq 3 yields pK_a values of 7.4 ± 0.1 and 10.4 ± 0.2. The k_{lim}/K_d versus pH profile reports on kinetically influential ionizations in the free enzyme and free substrate forms, and the bell-shaped dependence is entirely due to changes in the dissociation constant for the enzyme−substrate complex (Table 1). The pK_a value of 10.4 ± 0.2 determined from the k_{lim}/K_d versus pH profile is similar to

[4] The pK_a values for the carboxyl and secondary amine groups of sarcosine are 2.23 and 10.01, respectively.

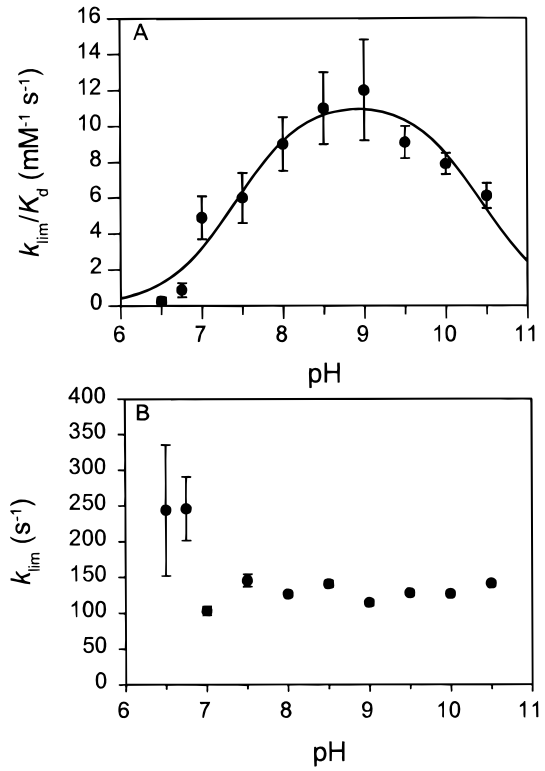

FIGURE 6: pH dependence of flavin reduction in sulfite-treated TSOX. Panel A: Plot of k_{lim}/K_d as a function of pH. Data are fitted to the expression for a double ionization (eq 3). Macroscopic pK_a values are 7.4 ± 0.1 and 10.4 ± 0.2. The data shown were also analyzed using the logarithmic form of eq 3 (not shown). Analysis using the logarithmic form provides for more appropriate weighting of points not located near the optimum of the plot shown in panel A. In this case, the upper pK_a has a value of 10.4 ± 0.5, the larger error reflecting the fact that no data are available above pH 10.5. Panel B: Plot of limiting electron-transfer rate constant, k_{lim}, as a function of pH. Data illustrate no apparent dependence on pH across the pH range investigated. The buffer range was achieved using phosphate, pyrophosphate, and borate buffers.

Table 1: Limiting Rate Constants for Flavin Reduction and Enzyme−Substrate Dissociation Constants for the Reaction of Sulfite-Treated TSOX with Sarcosine

pH	k_{lim} (s^{-1})	K_d (mM)	k_{lim}/K_d (mM^{-1}·s^{-1})
6.5	244 ± 92	940 ± 400	0.26 ± 0.21
6.75	246 ± 45	283 ± 77	0.87 ± 0.39
7.0	103 ± 6	21 ± 4	4.9 ± 1.2
7.5	145 ± 9	24 ± 4	6.0 ± 1.4
8.0	126 ± 3	14 ± 2	9.0 ± 1.5
8.5	141 ± 5	13 ± 2	11 ± 2.0
9.0	115 ± 5	10 ± 2	12 ± 2.8
9.5	128 ± 3	14 ± 1	9.1 ± 0.9
10.0	127 ± 2	16 ± 1	7.9 ± 0.6
10.5	141 ± 3	23 ± 2	6.1 ± 0.7

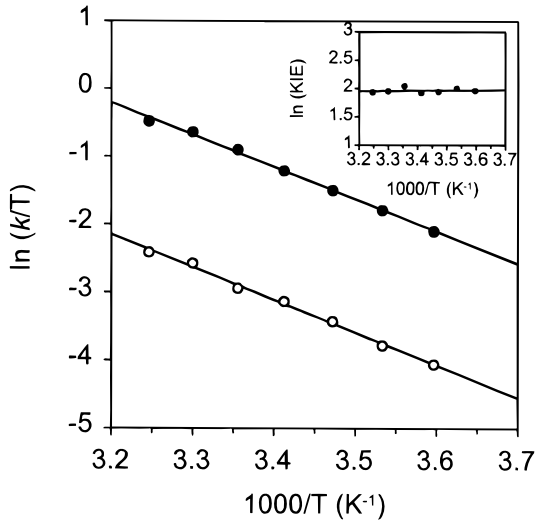

FIGURE 7: Temperature dependence and KIE data for sulfite-treated TSOX. Main panel: Temperature dependence plots with sarcosine (filled circles) and *N*-methyl-d_3-glycine hydrochloride (deuterated sarcosine) (open circles). $\ln(A'^{H}) = 14.9 \pm 0.4$, $\ln(A'^{D}) = 13.2 \pm 0.5$, $\Delta H^{H} = 39.4 \pm 0.9$ kJ mol^{-1}, $\Delta H^{D} = 40.0 \pm 1.2$ kJ mol^{-1}. Inset: Plot of ln(KIE) versus 1/*T*. The error for rates measured at all temperatures is less than 4% of the determined values.

the known value of the pK_a for the secondary amine group in sarcosine (pK_a = 10.0).[4] A possibility, therefore, is that the value of 10.4 ± 0.2 represents the ionization of this group in sarcosine, although the ionization of a group on the protein cannot be ruled out. The pK_a value of 7.4 ± 0.1 on the acid limb of the bell-shaped curve is attributed to an ionization in TSOX, since the value is substantially greater than the carboxylate group of sarcosine (pK_a = 2.2).

Kinetic Isotope Studies of C−H Bond Breakage by TSOX. The rate of flavin reduction with sarcosine and *N*-methyl-d_3-glycine hydrochloride was studied at 25 °C and pH 8.5 at sarcosine and *N*-methyl-d_3-glycine concentrations of 150 mM (i.e., greater 10 × K_d). These investigations revealed a KIE of 7.3 on the flavin reduction step, demonstrating that C−H bond cleavage is rate-limiting for flavin reduction (Figure 7). The temperature dependence of the rate constant (*k*) for flavin reduction was also investigated. The temperature dependence for a unimolecular rate constant is given by eq 4:

$$k = \frac{k_B}{h} T e^{-\Delta G^{\ddagger}/RT} = \frac{k_B}{h} T e^{-\Delta H^{\ddagger}/RT} e^{\Delta S^{\ddagger}/R} \qquad (4)$$

where k_B and *h* are the Boltzmann and Planck constants, respectively. A convenient way of plotting the temperature dependence of a unimolecular reaction is to use eq 5:

$$\ln(k/T) = \ln(k_B/h) + \Delta S^{\ddagger}/R - \Delta H^{\ddagger}/RT \qquad (5)$$

The activation parameter $\Delta H^{\ddagger}$ is calculated from the slope of the plot. $\Delta S^{\ddagger}$ is calculated by extrapolation to the ordinate axis, and $\Delta G^{\ddagger}$ is then calculated directly from eq 4. Analysis of the temperature dependence of k_{lim} using eq 5 is illustrated in Figure 7. The data indicate that the KIE is independent of temperature and that the difference in the enthalpy of activation for protium versus deuterium transfer ($\Delta\Delta H^{\ddagger} = \Delta\Delta H^{\ddagger D} - \Delta\Delta H^{\ddagger H} = 0.6 \pm 2.1$ kJ mol^{-1}) is essentially zero. The value of the A'^{H}:A'^{D} ratio (5.8) calculated from the intercepts of the plots is similar to that of the KIE (7.3). As discussed previously (*19*), the use of eq 5 in plotting the temperature dependence of a unimolecular reaction is preferred over the use of the classical Arrhenius plot that has been adopted by other workers. This arises because the Arrhenius equation is actually curved (although it appears linear in the accessible temperature range) and asymptotically approaches infinity at high temperatures. A necessary consequence of using eq 5 (rather than the Arrhenius equation that has been used by other workers to identify tunneling regimes) is the need to define explicitly the meaning of values obtained from such plots. Use of the Arrhenius plot has led to the development of criteria to indicate tunneling based on the values for $\Delta\Delta E_a$ and the A^H:A^D ratio (calculated from the intercepts of the Arrhenius plot for protium and deuterium substrates). The corresponding parameters calculated from the slopes and intercepts of plots using eq 5 are $\Delta\Delta H^{\ddagger}$and A'^{H}:A'^{D} (the prime is used to distinguish this ratio from the A^H:A^D ratio calculated from the classical Arrhenius plot). Observations similar to those discussed above for the temperature-dependent behavior of C−H bond breakage in TSOX have been made during cleavage of a substrate C−H bond by the TTQ-dependent methylamine dehydrogenase (MADH) of *Methylophilus methylotrophus.* For MADH, the data were interpreted in terms of ground-state tunneling of protium and deuterium through a fluctuating potential energy barrier (*19*). Our data for the reaction catalyzed by TSOX suggest that ground-state tunneling of protium and deuterium also occurs during C−H and C−D bond cleavage and that tunneling is driven by the thermal motion of the protein scaffold (*26, 27*). A more detailed appraisal of these results is presented under Discussion.

DISCUSSION

In this paper, we have examined the mechanism of substrate C−H bond breakage and the kinetics of flavin reduction in the reaction of TSOX with its natural substrate sarcosine. The ability to selectively form a flavin−sulfite adduct with the covalent 8α-(N^3-histidyl)-FMN has enabled us to study in detail the kinetics of substrate oxidation at the site of the noncovalent FAD using stopped-flow methods. The pH profile for k_{lim} reveals that there are no kinetically influential ionizations in the enzyme−substrate complex in the pH range 6.5−10. However, a bell-shaped dependence on pH for k_{lim}/K_d is observed, reflecting two ionizations either in the free enzyme and/or in the free substrate forms. The macroscopic pK_a values for these ionizations are 7.4 ± 0.1 and 10.4 ± 0.2, and these ionizations exert their effect on the enzyme−substrate dissociation constant, K_d (Table 1). The assignment of these ionizations to functional groups in the enzyme or substrate is of interest, but the lack of a structural solution for TSOX prevents detailed analysis. However, the β-subunit of TSOX exhibits modest sequence identity (23%) with the structurally determined MSOX of *Bacillus* sp. B-0618 (*6*), and all of the residues implicated in catalysis by MSOX are conserved in βTSOX. Useful comparisons can therefore be made between the two enzyme molecules. The structure of MSOX has been solved in the presence of two inhibitors, (methylthio)acetic acid (MTA) and pyrrole-2-carboxylic acid (PCA), and these structures provide insight into the mode by which sarcosine binds to MSOX. The structural analysis suggests that the binding of

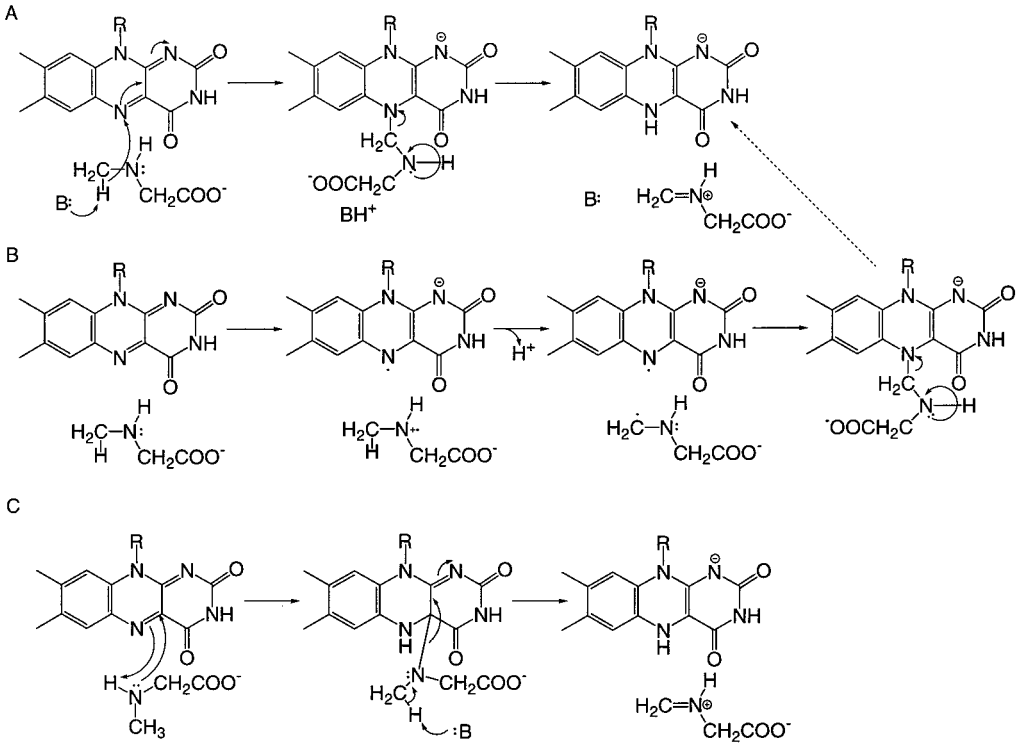

FIGURE 8: Potential mechanisms for the oxidation of sarcosine by TSOX. Mechanism A: The carbanion mechanism involving proton abstraction and the formation of a transient covalent intermediate between the carbanion and the flavin N5. Mechanism B: The SET amminium radical cation mechanism originally proposed for monoamine oxidase and adapted for sarcosine oxidase. Mechanism C: Nucleophilic attack by the substrate nitrogen at the flavin C4a atom, followed by proton abstraction by an active site base. Another potential mechanism not shown includes the hydride anion transfer mechanism, involving the direct transfer of a hydride anion from the substrate methyl group to the flavin N5 atom. All the mechanisms shown above are illustrated with the sarcosine amine group unprotonated. At physiological pH, the amine group will be protonated, and thus deprotonation of this group in the enzyme−substrate complex would be required for each mechanism illustrated.

sarcosine is probably stabilized by hydrogen bonds between the substrate carboxylate and two basic side chains, Arg-52 and Lys-348 (both conserved in βTSOX), which are located above the *re* face of the flavin (*6*). Thus, the pK_a value of 10.4 ± 0.2 observed in our experiments with TSOX might represent the ionization of, for example, the βTSOX counterpart of Lys-348 found in MSOX. Alternatively, this ionization may represent that of the methylated amine group of sarcosine itself (pK_a 10.01). The ionization on the acid side of the bell-shaped curve (pK_a = 7.4 ± 0.1) is most likely protein-based, since the carboxylate group of sarcosine ionizes with a pK_a value of 2.23. Inspection of the crystallographic structure of MSOX suggests that the βTSOX counterpart of His-269 found in MSOX is a candidate for the ionizable group of pK_a = 7.4. Using the known structures of MSOX complexed with MTA and PCA as a guide, His-269 would be located close to the methylated amine group of sarcosine in MSOX (and thus, by analogy, in βTSOX). It is expected that protonation of this histidine residue would raise the enzyme−substrate dissociation constant by juxtaposing the positive charges of its imidazole side chain with the protonated amine group of sarcosine. Although the structure of MSOX solved in the presence of MTA and PCA provides useful insight, formal identification of the ionizable groups awaits further analysis by site-directed mutagenesis.

Our pH-dependent kinetic data for TSOX need to be considered in light of proposed mechanisms of amine oxidation by flavoenzymes. The reaction involves the cleavage of a substrate C−H bond, and in principle this can occur in a variety of ways (Figure 8). Direct H-abstraction from the substrate methyl group involving an amino acid radical as a H· acceptor can be ruled out, since EPR studies indicate the lack of a radical species in the resting enzyme. However, bond breakage can be achieved by a variety of other mechanisms. These include a direct hydride transfer from the methyl group to the flavin N5 atom (mechanism not shown), which has been proposed for many flavoprotein-catalyzed oxidations. Proton abstraction via an active site base (the so-called carbanion mechanism; Figure 8, mechanism A) or a single electron transfer (SET) mechanism, as originally proposed for monoamine oxidase (*17*) (Figure 8, mechanism B), is also possible. Additionally, an alternative mechanism, originally proposed for monoamine oxidase (*28*), should be considered. This mechanism involves direct nucleophilic attack of the substrate nitrogen at the flavin C4a atom (Figure 8, mechanism C). Similar mechanisms have been discussed in relation to the oxidation of trimethylamine by trimethylamine dehydrogenase (TMADH) (*16*). Our kinetic investigations with TSOX reveal that there are no kinetically influential ionizations in the enzyme−substrate complex within the range pH 6.5−10. However, this observation does not exclude a carbanion mechanism—which has a requirement for an active site base—since any such base may have a pK_a below pH 6.5 and/or there may be hindered exchange of a proton between solvent and an active site base. For the same reasons, the lack of a kinetically influential ionization in the k_{lim} versus pH profile does not eliminate the functioning of a base required for the operation of mechanism C shown in Figure 8. All the mechanisms shown in Figure 8 require the unprotonated form of the

amine. However, at physiological pH values, sarcosine is protonated (pK_a 10.01). Thus, if any of the mechanisms were to account for sarcosine oxidation by TSOX, there would need to be a deprotonation of the amine group (the deprotonated form is shown in Figure 8) in the enzyme−substrate complex. Our kinetic data can thus not rule out unequivocally any of the mechanisms shown in Figure 8, or indeed the direct hydride transfer mechanism. Thus, such as with TMADH (*16*), the precise mechanism of C−H bond cleavage by TSOX remains to be established, but our kinetic studies have identified important ionizations that will be the focus of future studies by site-directed mutagenesis.

Flavin reduction by sarcosine is associated with a KIE of 7.3. This value is toward the upper limit for semiclassical behavior if the reaction catalyzed by TSOX is modeled using the static potential energy barrier depictions of transition state theory (TST) (*29*). Examination of the temperature dependence of the reaction by stopped-flow methods, however, indicates the reaction is nonclassical, as evidenced by the A'^{H}:A'^{D} ratio >1 (see ref *19* for a definition of A'^{H}:A'^{D} ratio). The observed behavior—i.e., essentially temperature-independent KIE over the experimental temperature range,[5] but large enthalpies of activation for the reaction (∼40 kJ mol^{-1})—is similar to that seen first in TTQ-dependent MADH (*19*) and subsequently in a thermophilic alcohol dehydrogenase (*30*). Although quantum tunneling of hydrogen has been documented in several enzyme molecules (e.g., see refs *31*−*35*), the experiments with MADH and thermophilic alcohol dehydrogenase have provided the first experimental evidence for a link between protein dynamics and H-tunneling. With MADH and the thermophilic alcohol dehydrogenase, the observed kinetic behavior was interpreted to indicate ground-state tunneling of hydrogen and deuterium through a fluctuating potential energy barrier, with the dynamic nature of the potential energy barrier arising from the low-frequency thermal motions of the protein molecule. Importantly, these dynamic barrier models of enzymatic H-tunneling can accommodate KIEs of <7 (i.e., the semiclassical region of the static barrier models) in a ground-state quantum tunneling regime (*18*). The fluctuating barrier model of catalysis is consistent with theoretical treatments of enzymatic H-tunneling (*18*) and has been reviewed recently with particular reference to enzymes where vibrationally enhanced ground-state tunneling (VEGST) has been demonstrated experimentally (*26, 27*). However, it is important to bear in mind that there are potential complications arising from our isotope studies with TSOX. Explicitly, these are (i) the issue of kinetic complexity and (ii) the magnitude of secondary isotope effects arising from perdeuteration of the substrate methyl group. First, as regards kinetic complexity, it is important to note that in our work with TSOX we have monitored flavin reduction by the stopped-flow technique to measure the rate of C−H bond cleavage. Since the precise mechanism of amine oxidation by TSOX is as yet unresolved, the question of whether the rate of flavin reduction is also a true indicator of the rate of C−H bond cleavage remains to be established. In this situation, it is possible, with decreasing temperature, that the expected increase in KIE (for semiclassical behavior) is offset by a decrease in kinetic commitment, leading to an observed KIE that is apparently independent of temperature, as described by eq 6:

$$\frac{{}^{H}k_{obs}}{{}^{D}k_{obs}} = \frac{\left(\frac{{}^{H}k_{int}}{{}^{D}k_{int}} + C\right)}{(1 + C)} \qquad (6)$$

where C is a ratio of rate constants reflecting the degree by which C−H bond breakage is rate-determining, ${}^{H}k_{obs}/{}^{D}k_{obs}$ is the observed KIE, and ${}^{H}k_{int}/{}^{D}k_{int}$ is the intrinsic KIE (*36*). Such arguments are commonplace in steady-state kinetic analyses, where passage over multiple potential energy barriers takes place. In single-turnover stopped-flow studies, which focus on 'one step' of the reaction, the rate of substrate oxidation/flavin reduction may in fact reflect more than one kinetic step, giving rise to internal commitments. However, in our opinion the following three factors combine to argue against internal commitments in our stopped-flow studies with TSOX, although unequivocal demonstration will require further work: (i) the analogous temperature-dependent kinetic behavior of TSOX, MADH [which is known to catalyze C−H bond breakage by VEGST (*19*)], and TMADH (Basran, Sutcliffe, and Scrutton, unpublished data); (ii) the fact that MADH, TMADH, and TSOX catalyze similar reactions (i.e., amine oxidation via C−H bond breakage); and (iii) the improbability of a perfectly matched compensatory change in intrinsic KIE and internal commitment yielding an observed KIE that is independent of temperature for both TSOX and TMADH. Second, an *upper* limit for secondary KIEs of 1.36 (*37*) for the perdeuterated methyl group of sarcosine may complicate the analysis if the full secondary KIE is realized. Thus, although our stopped-flow data provide strong indications for a VEGST mechanism in TSOX, future studies will need to address these two aspects with respect to the TSOX-catalyzed oxidation of amines to prove unequivocally a role for VEGST of hydrogen during C−H bond cleavage.

CONCLUSIONS

We have demonstrated that the reduction of FAD bound by *Arthrobacter* TSOX can be examined in the absence of internal electron transfer and oxidase activity by sulfite treatment of the enzyme. The limiting rate of FAD reduction is independent of solution pH (between 6.5 and 10.5), indicating the lack of participation of an active site base in bond cleavage in the accessible pH range. Substrate binding is influenced by two kinetically influential ionizations of pK_a 7.4 and 10.2. The pH dependence studies of FAD reduction are consistent with many of the mechanisms for the flavin-dependent oxidation of amines proposed previously in the

[5] Theory predicts that for ground-state tunnelling of hydrogen through a fluctuating potential energy barrier, the ln(KIE) displays a parabolic dependence on 1/T when the quantum mechanical transfer is rate-limiting (*18*). However, these complex dependencies will only be apparent over an extended temperature range, which is not accessible in studies with enzyme molecules. Therefore, over the restricted temperature range used in studies with TSOX, there is an apparent independence of ln(KIE) on 1/T. At lower temperatures, the ln(KIE) versus 1/T plot for TSOX would be expected to turn upward, in line with the predicted parabolic dependence. However, it is also important to note that at cryogenic temperatures nuclear reorganization of the protein scaffold may become rate-limiting—under these conditions, the KIE will tend toward unity, and the parabolic dependence will be lost because of the reduced thermal motions in the protein scaffold.

literature. Kinetic isotope effect studies indicate that VEGST is the likely mechanism of H-transfer during breakage of the substrate C−H bond.

REFERENCES

1. Suzuki, K., Sagai, H., Imamura, S., and Sugiyama, M. (1994) *J. Ferm. Biol. 77*, 231−234.
2. Koyama, Y., Yamamoto-Otake, H., Suzuki, M., and Nakano, E. (1991) *Agric. Biol. Chem. 55*, 1259−1263.
3. Chlumsky, L. J., Zhang, L., and Jorns, M. S. (1995) *J. Biol. Chem. 270*, 18252−18259.
4. Suzuki, K., Ogishima, M., Sugiyama, M., Inouye, Y., Nakamura, S., and Imamura, S. (1992) *Biosci. Biotechnol. Biochem. 56*, 432−436.
5. Reuber, B. E., Karl, C., Reimann, S. A., Mihalik, S. J., and Dodt, G. (1997) *J. Biol. Chem. 272*, 6766−6776.
6. Trickey, P., Wagner, M. A., Jorns, M. S., and Mathews, F. S. (1999) *Structure 7*, 331−345.
7. Mattevi, A., Vanoni, M. A., Todone, F., Rizzi, M., Teplyakov, A., Coda, A., Bolognesi, M., and Curti, B. (1996) *Proc. Natl. Acad. Sci. U.S.A. 93*, 7496−7501.
8. Kvalnes-Krick, K., and Jorns, M. S. (1986) *Biochemistry 25*, 6061−6069.
9. Willie, A., and Jorns, M. S. (1995) *Biochemistry 34*, 16703−16707.
10. Chlumsky, L. J., Sturgess, A. W., Nieves, E., and Jorns, M. S. (1998) *Biochemistry 37*, 2089−2095.
11. Willie, A., Edmondson, D. E., and Jorns, M. S. (1996) *Biochemistry 35*, 5292−5299.
12. Kvalnes-Krick, K., and Jorns, M. S. (1987) *Biochemistry 26*, 7391−7395.
13. Jorns, M. S. (1985) *Biochemistry 24*, 3189−3194.
14. Zeller, H. D., Hille, R., and Jorns, M. S. (1989) *Biochemistry 28*, 5145−5154.
15. Ali, S. N., Zeller, H. D., Calisto, M. K., and Jorns, M. S. (1991) *Biochemistry 30*, 10980−10986.
16. Jang, M.-H., Basran, J., Scrutton, N. S., and Hille, R. (1999) *J. Biol. Chem. 274*, 13147−13154.
17. Silverman, R. B. (1995) *Acc. Chem. Res. 28*, 335−342.
18. Bruno, W. J., and Bialek, W. (1992) *Biophys. J. 63*, 689−699.
19. Basran, J., Sutcliffe, M. J., and Scrutton, N. S. (1999) *Biochemistry 38*, 3218−3222.
20. Sambrook, J., Fritsch, E. F., and Maniatis, T. (1989) *Molecular cloning: a laboratory manual*, 2nd ed., Cold Spring Harbor Laboratory Press, Cold Spring Harbor, NY.
21. Meskys, R., Rudomanskis, R., and Leipuviene, R. (1996) *Biotech. Lett. 18*, 781−786.
22. Mewies, M., McIntire, W. S., and Scrutton, N. S. (1998) *Protein Sci. 7*, 7−20.
23. Strickland, S., Palmer, G., and Massey, V. (1975) *J. Biol. Chem.*, 4048−4052.
24. Chlumsky, L. J., Zhang, L., Ramsey, A. J., and Jorns, M. S. (1993) *Biochemistry 32*, 11132−11142.
25. Kawamura-Konishi, Y., and Suzuki, H. (1987) *Biochim. Biophys. Acta 915*, 346−356.
26. Scrutton, N. S., Basran, J., and Sutcliffe, M. J. (1999) *Eur. J. Biochem. 264*, 666−671.
27. Sutcliffe, M. J., and Scrutton, N. S. (1999) *Philos. Trans. R. Soc., Ser. A* (in press).
28. Kim, J.-M., Bogdon, M. A., and Mariano, P. S. (1993) *J. Am. Chem. Soc. 115*, 10591−10595.
29. Bell, R. P. (1980) in *The Tunnel Effect in Chemistry*, pp 51−140, Chapman and Hall, London.
30. Kohen, A., Cannio, R., Bartolucci, S., and Klinman, J. P. (1999) *Nature 399*, 496−499.
31. Cha, Y., Murray, C. J. and Klinman, J. P. (1989) *Science 243*, 1325.
32. Jonsson, T., Edmondson, D. E. and Klinman, J. P. (1994) *Biochemistry 33*, 14871.
33. Kohen, A., Jonsson, T., and Klinman, J. P. (1997) *Biochemistry 36*, 2603.
34. Grant, K. L., and Klinman, J. P. (1989) *Biochemistry 28*, 6597.
35. Jonsson, T., Glickman, M. H., Sun, S. J., and Klinman, J. (1996) *J. Am. Chem. Soc. 118*, 10319.
36. Schimerlik, M. I., Grimshaw, C. E., and Cleland, W. W. (1977) *Biochemistry 16*, 571−576.
37. Klinman, J. P. (1978) *Adv. Enzymol. Relat. Areas Mol. Biol. 46*, 415−494.

BI991941V